Histol Histopathol (2013) 28: 89-100
DOI: 10.14670/HH-28.89

http://www.hh.um.es

Histology and Histopathology
Cellular and Molecular Biology

New serum-derived albumin scaffold seeded with adipose-derived stem cells and olfactory ensheathing cells used to treat spinal cord injured rats

Amaia Ferrero-Gutierrez[1]*, Yolanda Menendez-Menendez[1]*, Maria Alvarez-Viejo[1], Alvaro Meana[2] and Jesus Otero[1]

[1]Transplant and Cell Therapy Unit. Hospital Universitario Central de Asturias, Oviedo, Spain and [2]Tissue Engineering Research Unit, Centro Comunitario de Sangre y Tejidos de Asturias, Oviedo, Spain. U714 Ciber Enfermedades Raras (CIBERER).

*These authors have contributed equally to this work.

Summary. Recent advances in spinal cord injury (SCI) research and cell culture techniques and biomaterials predict promising new treatments for patients with SCI or other nerve injuries. Biomaterial scaffolds form a substrate within which cells are instructed to form a tissue in a controlled manner. This study was designed to assess axon regeneration and locomotor recovery in rats with spinal cord injury treated with a novel serum-derived albumin scaffold seeded with adipose derived stem cells (ADSCs) and olfactory ensheathing cells (OECs). OECs are considered promising candidates for the treatment of SCI, and ADSCs have the ability to differentiate into neural lineages. *In vitro* experiments revealed that ADSCs and OECs adhered to the scaffold, remained viable and expressed specific markers of their cell types when cultured in the scaffold. Rats treated with scaffold plus cells showed locomotor skills at several time points from 45 days post-injury that were improved over those recorded in control injured, untreated animals. Astrocytic scars and tissue regeneration, identified using histological and immunohistochemical techniques, revealed that although the scaffold itself appeared to play a significant role in reducing glial scar formation and filling of the lesion cavity with cells, the presence of ADSCs and OECs in the scaffold led to the appearance of cells expressing markers of neurons and axons at the injury site. Our findings point to the clinical feasibility of an albumin scaffold seeded with ADSCs and OECs as a treatment candidate for use in spinal cord injury repair studies.

Key words: Spinal cord injury, Cell transplantation, Albumin scaffold, Adipose-derived stem cells (ADSCs), Olfactory ensheathing cells (OECs)

Offprint requests to: Amaia Ferrero-Gutierrez, Laboratorio de Trasplantes y Terapia Celular, Hospital Universitario Central de Asturias, (HUCA), c/ Celestino Villamil s/n, Edificio Polivalente A, 1ª Planta, 33006 Oviedo, Asturias, Spain. e-mail: amaya.ferrero@sespa.princast.es

Introduction

Spinal cord injury (SCI) is a devastating condition that generally produces partial or complete sensory and motor loss below the level of injury. Immediately after SCI, axonal structural and electrophysiological abnormalities can be seen in both gray and white matter (Balentine, 1978). Trauma causes the death of neurons and glial cells as well as axon tract injury. Since dead neurons are not replaced and injured axons are not spontaneously regenerated, functional disorders are permanent (Cadelli et al., 1992; Schwab and Caroni, 2008). The lesion site produced by SCI poses many obstacles for promoting tissue and cell regeneration. Events subsequent to SCI include the formation of a cystic cavity at the injury site, which becomes surrounded by a glial and fibrous scar, composed of mainly reactive astrocytes, thus generating a physical barrier to spontaneous regeneration (Fawcett and Asher, 1999; Brazda and Müller, 2009). In addition, the demyelination that occurs after SCI produces several inhibitory molecules and signals that contribute to this lack of regeneration (McGee and Strittmatter, 2003; Busch and Silver, 2007).

Preliminary empirical experiments designed to either maintain or recover neuronal functions have focused on regenerating injured axons and replacing lost neurons by cell transplantation (Li et al., 2004; Wang et al., 2006).

Good candidates for cell transplant-mediated repair of central nervous system lesions are glial cells, such as olfactory ensheathing cells (OECs) (Raisman, 2001; Barnett and Riddell, 2004). OECs are capable of migrating into and through astrocytic scars and thereby facilitate axonal regrowth, promoting neural regeneration and functional reconstruction (Raisman, 1985). *In vitro* and *in vivo* studies have shown that the injection of OECs at the injury site creates a favorable environment for the regeneration and remyelination of central cord axons, and may even achieve functional recovery in animal models of SCI (Groves et al., 1993; Ramon-Cueto et al., 1998; Radtke et al., 2009). OEC transplantation is however limited by the availability of functional cells. A promising new cell strategy is based on the use of adult mesenchymal stem cells (MSC). Adipose-derived stem cells (ADSCs) are able to differentiate towards a neuronal phenotype *in vitro* as well as *in vivo*, and the possible use of these cells to treat neurological disorders has attracted the attention of researchers (Kang et al., 2003). Although the injection of OECs directly into the site of SCI seems to be of limited use (Resnick et al., 2003; Collazos-Castro et al., 2005), some of the neurotrophic factors secreted by OECs have been successfully used to induce MSC differentiation into neurons and glial cells *in vitro* (Jin et al., 2003; Tatard et al., 2007). However, other authors (Zhang et al., 2009; Arboleda et al., 2011) show that the functional improvement in animals with SCI transplanted with MSCs may be caused by the release of trophic factors via a paracrine effect.

Biodegradable polymer scaffolds serve to form a structural support to bridge the injury site and guide axon regeneration (Olson et al., 2009; Straley et al., 2010). The scaffold used in the present study was a biodegradable cross-linked plasma-based matrix that serves as a three-dimensional substrate. An essential benefit of this new scaffold is that it is prepared from the patient's own blood and can be used as an autologous scaffold, avoiding the risks of foreign body reaction or infection (Gallego et al., 2010). In effect, this new scaffold could have many tissue-engineering applications, and in previous experimental studies we described its successful use to repair bone defects (Gallego et al., 2009, 2010).

The present study was designed to assess the effect of a combination of adipose derived stem cells (ADSCs) and olfactory ensheathing cells (OECs) seeded in a novel serum-derived albumin scaffold on SCI.

Materials and methods

Scaffold preparation

The scaffold was elaborated as previously described (Meana et al., 2008; Gallego et al., 2010) according to patent WO2008/119855. In brief, 10 ml of human venous blood was obtained from a blood bank and kept for 30 min at 37°C. Next, the blood was centrifuged for 15 min at 2000 g and the resultant serum (5 ml) was crosslinked with 0.5 ml 25% glutaraldehyde (Merck, Darmstadt, Germany) and transferred to a 5 ml disposable syringe. After keeping the serum/glutaraldehyde solution at room temperature for 30 min until solidification, it was frozen and kept at -70°C overnight. Next the syringe was cut open and the frozen solution was lyophilized for 48 h and rehydrated in a graded ethanol series (100-90-80%) by immersing for 1 h in each dilution. The tube-shaped scaffold obtained was then cut into 3 mm-diameter, 1-2 mm-thick sections and sterilized in 70% ethanol for 8 h. Finally, these small tubes of scaffold were neutralized in Dulbecco's modified Eagle's medium (DMEM; Gibco Invitrogen, Paisley, United Kingdom). Before cell seeding, excess fluid was removed and the scaffolds were placed in a 24-well culture plate (Nunc, Darmstadt, Germany) as one scaffold per well.

Adipose-derived stem cell (ADSCs) cultures

1-2 g of abdominal mesenteric adipose tissue was obtained from Wistar rats under anesthesia induced by isoflurane inhalation (Esteve laboratories, Milan, Italy), washed three times in phosphate-buffered saline (PBS; PAA Laboratories GmbH, Cölbe, Germany), chopped and placed in a test tube. After adding 0.1% collagenase I (Sigma-Aldrich, Madrid, Spain) in DMEM (Gibco Invitrogen), the suspension was shaken and digested for 1 h at 37°C. Digestion was stopped by adding fetal bovine serum (FBS; Gibco Invitrogen). After filtering through a 0.40 μm cell strainer (BD Bioscience, Madrid, Spain) and centrifuging at 500 g for 10 min, the cells were seeded on 25 cm^2 polystyrene flasks (Cultek, Madrid, Spain) in an ADSCs culture medium consisting of low-dose sugar DMEM (Gibco Invitrogen) supplemented with 10 % FBS, 100 U/ml penicillin (Gibco Invitrogen), and 100 μg/ml streptomycin (Gibco Invitrogen). Cells were cultured in a controlled atmosphere (37°C, 5% CO_2) at 48 h, the medium was first replaced and unattached cells removed. Thereafter, the medium was replenished every 2-3 days, and on the 14^{th} day, when confluent, the cells were digested with trypsin (0.25 % w/v; Gibco Invitrogen) and passaged four times before their use.

Olfactory ensheathing cells (OECs) cultures and purification

Primary olfactory bulb (OB) cells from adult female Wistar rats (three months old; Harlan Laboratories, Germany) were cultured as described elsewhere in detail (Gudiño-Cabrera and Nieto-Sampedro, 1996). The method used to purify OECs from these primary OB cultures was modified from the original protocol (Ramon-Cueto and Nieto-Sampedro, 1994). Thus, 14 days after plating, OECs were separated from other cell types in primary cultures by immunoaffinity using an antibody against the p-75 nerve growth factor receptor

(p-75 NGFR; Chemicon, Millipore, Madrid, Spain) (1:1000). Cells from primary cultures were detached with 0.25% trypsin, centrifuged (200 g; 10 min), and incubated with the p-75 NGFR antibody for 45 min at room temperature. Next, the cells were washed twice in PBS/BSA/EDTA and incubated with monoclonal IgG attached to Dynabeads M-450 (DBM-450; magnetic beads, coated with goat anti-mouse IgG; Miltenyi Biotec, Madrid, Spain) for 30 min at 4°C. The cells were selectively attached to the magnetic beads and separated from the cells that did not express p75-NGFR with the help of a potent permanent magnet (69) to retain the magnetic bead-OEC complexes. These complexes were washed three times in PBS/BSA/EDTA and the OECs seeded onto a poly-L-lysine-treated (Sigma-Aldrich; average molecular weight, 30,000; 50 mg/ml) 25 cm^2 flask followed by incubation for 48 h in an OEC culture medium (1:1 mixture of DMEM and Ham's F-12 medium (Lonza, Barcelona, Spain) supplemented with 10% FBS, 100 U/ml penicillin, and 100 μg/ml streptomycin) at 37°C in a 5% CO_2 atmosphere.

Cell seeding

Confluent cultures of ADSCs (fourth passage) and OECs were trypsinized and counted in a Neubauer hemocytometer. The cells released were suspended in DMEM containing 10% FBS. Once the DMEM had been removed, the ADSCs and OECs were seeded in scaffold culture medium (DMEM containing 10% FBS, 100 U/ml penicillin and 100 μg/ml streptomycin plus 25 ng/ml NT-3 (Sigma) and 100 ng/ml NGF (Sigma-Aldrich)). Next, $1x10^6$ ADSCs (0.5 ml) and $5x10^5$ OECs (0.5 ml) were seeded onto the scaffolds in the wells. The scaffolds were kept under shaking for 48 h to allow the cells to attach. The culture medium was replenished twice per week. The cells were maintained for 7 days at 37°C in a humidified atmosphere of 5% CO_2.

In vitro experiments

The following *in vitro* study groups were established:
Scaffold control (n = 5): Scaffold alone.
Scaffold + ADSCs + OECs (n = 5): ADSCs and OECs co-cultured in the scaffold.

Scanning electron microscopy (SEM)

The structural features of the scaffold and cells in the scaffold (ADSCs and OECs) were observed by scanning electron microscopy. The scaffolds were fixed in 2% phosphate-buffered glutaraldehyde 0.1 M (Panreac, Barcelona, Spain) for 12 h. The fixed samples were dehydrated in a graded series of acetone (30-50-70-90-100%; Merck, Darmstadt, Germany) and subsequently dried at critical point using CO_2 (Baltec CDP 030 critical point dryer). These samples were sputter-coated with gold and then viewed by SEM (JEOL JSM 6100, Tokyo, Japan).

Assessment of nuclear morphology

The scaffolds were fixed overnight in 4% paraformaldehyde (Panreac) in 0.1 M PBS at 4°C. After washing twice in PBS, the scaffolds were frozen in isopentane (Merck) and embedded in OCT medium (Tissue-Tek, Zoeterwoude, Netherlands) and sections 5- to 10 μm-thick cut on a cryostat (model Jung friocut 2800E, Leica, Heerbrugg, Switzerland). The sections were placed in PBS and, finally, stained with the nuclear fluorescent dye DAPI (1.5 μg/ml) (Vectashield mounting medium with DAPI; Vector Laboratories, Peterborough, United Kingdom) and covered with coverslips. Observations and photographs were documented using an Olympus BX-41 fluorescence microscope coupled to a digital camera (model DP71; Olympus, Barcelona, Spain) and the results analyzed using the equipment's image analysis software.

Immunohistochemical analysis

The scaffolds were fixed overnight in 4% paraformaldehyde in 0.1 M PBS at 4°C, frozen in isopentane and embedded in OCT medium, and sections 5- to 10 μm-thick cut on a cryostat. For immunohistochemistry, the sections were mounted on glass slides, placed in PBS and endogenous peroxidase blocked after 30 min with 1% H_2O_2. Possible background staining was blocked by incubating sections for at least 30 min in 5% BSA (Merck) in PBS. Sections were then incubated with mouse anti-vimentin monoclonal antibody (Dako, Barcelona, Spain) (1:100) for 30 min at room temperature in a humid chamber or with mouse anti-p75 NGFR monoclonal antibody (Millipore) (1:200) for 18 h at 4°C in a humid chamber. After further rinsing in PBS, the sections were immediately incubated with the secondary antibody conjugated to peroxidase (Dako) for 30 min at room temperature in a humid chamber. The complexes antibody-vimentin and antibody-p-75 NGFR could then be localized using the REAL EnVision Detection system kit (Dako). This kit uses a 3'-3'-diaminobenzidine (DAB)-like chromogen, staining vimentin and p75-NGFR-positive cells brown. Labeled sections were mounted in a hydrophobic medium (Entellan; Merck). Other sections were stained with hematoxylin and eosin (H&E) for microscopy examination. Observations and photographs were documented using an Olympus BX-41 microscope coupled to a digital camera (Olympus) and the results analyzed using the equipment's image analysis software.

In vivo experiments

Spinal cord injury model

The SCI model used was that described by Demjen et al. (2004) in which injury is produced by severing the

cord using scissors to cut around the cord perimetry, but leaving a small hinge uncut (the cord is thus around 80% transected). This results in the formation of a central cavity although some axons are spared. Animals injured in this manner have symmetrical paraplegia and are incapable of hindlimb movement immediately after surgery. SCI was induced in female Wistar rats (Laboratory Animal Center, University of Oviedo, Oviedo, Spain), all matched for age (12 weeks old) and weight (mean 250 g). The rats were anesthetized by isoflurane inhalation (Esteve). Under aseptic conditions, the spinal cord was exposed by laminectomy at vertebral level T7, and then symmetrically injured as described above using fine iridectomy scissors (FST, Heidelberg, Germany). After SCI, the rats were randomly and blindly assigned to the different treatment groups. When the spinal cord is injured, the tissue contraction produced leaves enough room for scaffold insertion. The scaffolds were implanted at the site of spinal cord injury 5 min after injury (n=8 per group). Starting 1 hour after the operation, the rats were treated with enrofloxacine (8.5 mg/kg) once a day for 7 days and buprenorphine (0.01 mg/kg) once a day for 3 days. The bladders of the animals were emptied manually once a day until they had recovered autonomic bladder function. The rats were kept in a climate-controlled, pathogen-free animal house and subjected to a12 h light-dark cycle. Food and water were available *ad libitum*. Experiments were conducted in accordance with the guidelines of the European Union (86-609-EU) and Spanish regulations (BOE 67-8509-12, 1988). Experimental protocols were also approved by the Committee for Animal Care and Handling of the University of Oviedo.

Animal treatment groups

The following *in vivo* treatment groups were established:
Group 1 (G1), SCI-only: rats subjected to SCI left untreated.
Group 2 (G2), SCI + scaffold: rats subjected to SCI and then treated with a cell-free scaffold.
Group 3 (G3), SCI with cell seeded scaffold: rats subjected to SCI and then treated with a scaffold seeded with ADSCs and OECs.

Modified BBB test

Overall motor performance of the animals was assessed using the BBB locomotor rating scale with slight modifications (Basso et al., 1995). Rats were place on a methacrylate walkway 1 m long and 6.2 cm wide. The runway was placed on top of an inclined mirror (60° angle) to enable the observation of hind-limb movements. Each animal had to walk the runway three times. In each testing session, the animals were scored independently by two observers blind to the treatment (the test was performed in a double-blinded manner). Hind-limb locomotion was scored from 0 (no observable hind-limb movement) to 21 points (normal movement). The scale was modified if the sequence of recovering motor features was not the same as described in the original score: since rats are able to raise their tails early in the recovery process, an additional 0.5 points were given for a raised tail position (Demjen et al., 2004).

All animals groups were tested on day 0 after SCI and once per week thereafter until 13 weeks post injury. Rats were recorded using a video camera while being tested, and their performance was then scored on digitalized videos played at one-quarter speed. In every treated group, n=8 except in G2 on day 14 post-injury, the n was 3 due to audiovisual problems.

Histological and immunohistochemical analysis

The animals in the different treatment groups were sacrificed 90 days after surgery. Briefly, the animals were transcardially perfused with saline solution, followed by ice-cold 4% paraformaldehyde. The entire spinal cords were dissected and post-fixed for an additional 48-72 h in the same fixative. Next, the spinal cords were softened in EDTA solution (10%, Panreac) for 10 days with the EDTA solution replenished each day. The spinal cords were harvested and approximately 2 cm lengths centered at the injury site analyzed. After decalcification, the spinal cords were dehydrated in a graded series of ethanol dilutions and embedded in paraffin. Sections 20 μm thick were obtained using a microtome (model H310; Micron, Waldorf, Germany), deparaffinated in xylene, rehydrated in an ethanol series, and placed in PBS. Some of the sections were mounted on glass slides for histological observations after H&E and Sirius red staining. For immunohistochemical studies, the sections were exposed to 1% H_2O_2 for 30 min after rinsing in PBS to quench endogenous peroxidase activity. Before incubation with primary antibodies, possible background staining was blocked by incubating sections for al least 30 min in 5% BSA in PBS. When using the anti-tyrosine hydroxylase primary antibody, slides were first placed in boiling citrate buffer (pH 6) in a pressure cooker. The primary antibodies used were mouse anti-ß-III tubulin monoclonal antibody (1:30000; Sigma-Aldrich), mouse anti-glial fibrillary acidic protein (GFAP) polyclonal antibody (1:15000; BD Bioscience), mouse anti-dopamine ß-hydroxylase monoclonal antibody (1:5000; Millipore), mouse anti-ß-galactosidase polyclonal antibody (1:15000; Millipore), mouse anti-tyrosine hydroxylase monoclonal antibody (1:1000; Millipore), mouse anti-neurofilament 200 monoclonal antibody (1:5000, Sigma-Aldrich), and mouse anti-GAP-43 monoclonal antibody (1:5000; Santa Cruz Biotechnology, Heidelberg, Germany). The sections were incubated with these primary antibodies overnight at 4°C in a humid chamber. After further rinsing in PBS, the sections were immediately incubated with the secondary antibody conjugated to peroxidase (Dako) for 30 min at room temperature in a humid chamber. The antibody complex could then be localized

using the REAL EnVision Detection system kit (Dako). This kit uses a DAB-like chromogen. All sections were counterstained with hematoxylin. Labeled sections were mounted in a hydrophobic medium (Entellan; Merck). Observations and photographs were documented using a Olympus BX-41 microscope coupled to a digital camera (Olympus) and the results analyzed using the equipment's image analysis software.

Statistical analysis

For statistical analysis we used the program Graphpad InStat for Windows. Data for the different groups were compared by unpaired two-tailed one-way analysis of variance (ANOVA) or using a Student's t-test. Data are provided as means ± S.E.M. Figures only indicate significant differences relevant to the discussion of the data. The level of significance was set at $p<0.05$.

Results

Microstructure of the scaffold and morphology of ADSCs and OECs cultured in the scaffold

The surface features of the albumin scaffold were observed by SEM. ADSCs and OECs, recognized according to their morphology, could be seen adhered to the scaffold. The structure of the three-dimensional scaffold may be seen in Fig. 1A. Pore diameter ranged from 50 to 150 μm (Fig. 1). Thus, an irregular sized and shaped sheet-like structure was observed, and almost all pores were interconnected. This provides suitable spaces for cells to grow into the scaffold. SEM observation of the cells incubated in the scaffold for 7 days revealed that OECs and ADSCs adhered to the scaffold (Fig. 1B).

Survival and characteristics of ADSCs and OECs when cultured in the scaffold

The effect of the scaffold on cell viability was determined by DNA staining using DAPI. After incubating the ADSCs and OECs for 7 days in the scaffold, almost all cell nuclei (99±3%) had regular contours and were round and large in size, which is a characteristic of live cells (Fig. 2A,B).

Next, the cells were characterized by immunohistochemical staining for vimentin and p75. Almost all ADSCs were vimentin positive (Fig. 2D), and OECs were positive for p75 (Fig. 2E).

Locomotor function

The SCI model used was that described previously (Demjen et al., 2004) in which SCI causes symmetric paraplegia in the hind-limbs. We quantified multiple aspects of spontaneous locomotion using the modified BBB locomotor score (Basso et al., 1995). On day one after injury, no variations in scores were detected among the three groups of animals, with all animals suffering complete paraplegia and a lack of response to sensory stimuli to the hind-limbs (scores were 0). Between days 7 and 35 post-SCI, the modified BBB score recorded for the SCI with cell seeded scaffold group (G3) was slightly higher than the scores for the control groups (G1, SCI-only and G2, SCI + scaffold), although in no case was the difference significant. Notably, clinical progress and locomotor function at each time point from 45 days post-injury were significantly better in SCI with cell seeded scaffold rats, compared to controls: 6.3 ± 1.8 in SCI-only and 5.4 ± 2.2 in SCI + scaffold (Fig. 3). 45 days after treatment, SCI with cell seeded scaffold rats

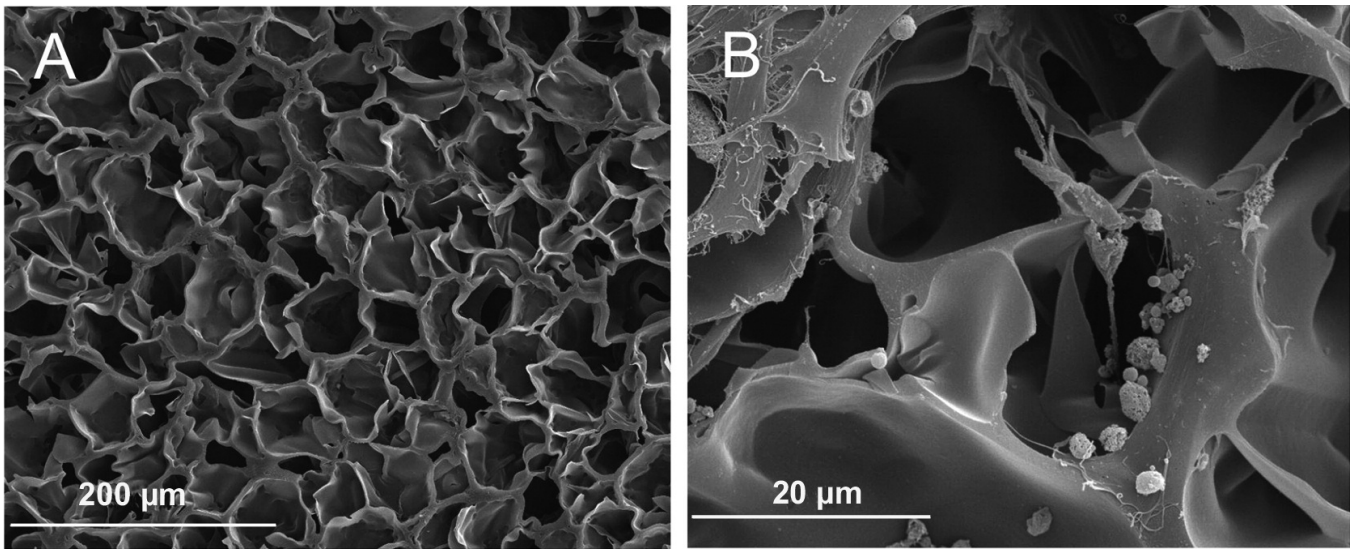

Fig. 1. Scanning electron microphotographs of cross sections showing the microstructure of: **(A)** the albumin scaffold, **(B)** adipose-derived stem cells (ADSCs) and olfactory ensheathing cells (OECs) adhered to the scaffold.

showed mean modified BBB scores of 8.3±0.2 (the maximum score of 21.5 indicates no motor defects). Thereafter, the scores tended to stabilize in the group, and mean score after 90 days of follow-up was 9.1±0.1. Scores for the control groups were similar to those recorded at 45 days: 5.7±0.6 and 4.3±1.1 respectively (Fig. 3). As may be seen in figure 3, no significant differences between control groups were observed at any of the treatment times. In short, overall locomotor recovery in the treatment group SCI with cell seeded scaffold was significantly better than in the control groups, as indicated by the slopes of plots of scores against time.

Histological analysis

To follow the course of spinal injury and the process of nervous tissue regeneration *in vivo*, histological studies were performed on all groups of animals after their sacrifice 90 days post-injury. Through H&E staining it was observed in SCI-only that the spinal cord central cavity had many areas empty of cells, although some zones were slightly filled with bundles of tissue, but there was no evidence of significant tissue regeneration (Fig. 4A). In contrast, in SCI + scaffold (Fig. 4B), and in SCI with cell seeded scaffold group (Fig. 4C) the cord central cavity was completely filled with cells 90 days post-injury. A visible reduction in the volume of residual scaffold was observed in the implant period, suggesting reabsorption of the scaffold and replacement with new tissue.

Sirius red was used to evaluate the extent of scar tissue formation. Thus, the site of injury was collagen positive in all animal groups at 90 days post-injury (see Table 1). This suggests that the motor improvement observed in SCI with cell seeded scaffold group was not

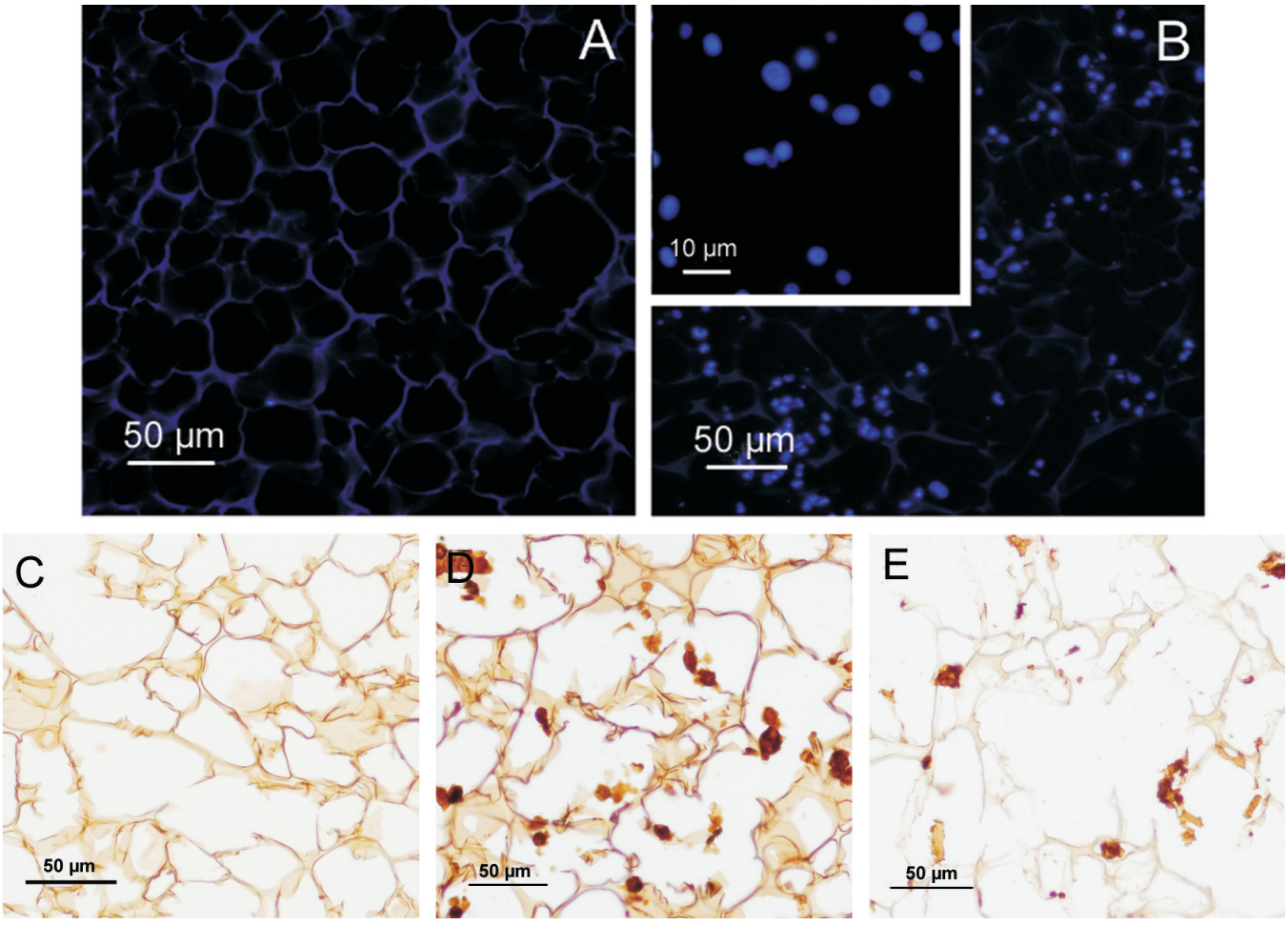

Fig. 2. Effect of the scaffold on the nuclear morphology of adipose-derived stem cells (ADSCs) and olfactory ensheathing cells (OECs). After incubating the cells in the scaffold for 7 days, cell nuclei were visualized by staining with the DNA-binding fluorescent dye DAPI. Note the autofluorescence of the scaffold in **(A). A.** Control (scaffold alone). **B.** Scaffold loaded with ADSCs and OECs. Immunocharacterizing the cell adipose-derived stem cells (ADSCs), and olfactory ensheathing cells (OECs) after 7 days of in vitro incubation in the scaffold. Control (scaffold alone) **(C)**, ADSCs stained with vimentin **(D)** and OECs stained with p75 **(E)**.

induced by collagen scar inhibition.

Immunohistochemical analysis

Once it had been established that the presence of scaffold plus cells did not inhibit collagen synthesis after SCI, we explored the classic concept of the formation of a glial scar in the injured spinal cord tissue using an antibody against the astrocyte marker GFAP. The results of this analysis indicate that rats in group SCI with cell seeded scaffold 90 days post-injury showed GFAP-negative cells filling the cord cavity and close to the injury site (rostral and caudal) (Fig. 5E), whereas SCI-only rats were GFAP-positive at sites immediately (rostral and caudal) next to the point of injury, which confirms the presence of glial scar in this control group (Fig. 5A). In contrast, cord cells in SCI + scaffold were negative for GFAP-immunostaining at the lesion site (images not shown). These observations suggest that the scaffold alone was able to inhibit glial scar formation and that the scaffold plus cells also suppressed this glial scar.

To assess the origin of newly formed tissue in the spinal cord cavities of the treatment groups, we used different specific antibodies. To determine whether or not the newly formed tissue could act as a bridge that permitted the passage of ascending and descending axons, we determined axons expressing tyrosine hydroxylase, neurofilament 200, dopamine ß-hydroxylase and GAP-43, as possible components of regeneration (see Table 1). Thus, SCI with cell seeded scaffold showed positive immunostaining for antibodies against tyrosine hydroxylase and neurofilament 200 inside and around the scaffold (images not shown). Similarly, cells in the cords of the SCI with cell seeded scaffold animals were GAP-43 positive rostral to the scaffold (injury site). Thus, immunopositive staining in the space where the initial injury took place, which was filled with the cell-loaded scaffolds, suggests that the newly formed tissue contained neurons or neuronal elements. SCI-only cords were negative for tyrosine hydroxylase, neurofilament 200, and GAP-43 from rostral to caudal zones, including the injury site (Fig. 5B). In contrast, cord cells in SCI + scaffold animals exhibited very few neurofilament 200, tyrosine hydroxylase, and GAP-43 positive fibers at the injury site (images not shown). In all groups, cord cells were dopamine ß-hydroxylase negative at the injury site (images not shown).

Finally, to examine the presence of neural and astroglial cells at the site of injury, we immunolabeled neurons expressing ß-III tubulin (adult neurons), GAP-43 (neurons observed during developmental growth) and neurons and astroglial cells expressing ß-galactosidase (see Table 1). Cord cells in all the treatment groups showed immunopositive staining for the ß-III tubulin antibody, although there were very few ß-III tubulin-positive cells in SCI-only and SCI + scaffold groups compared to the SCI with cell seeded scaffold group (Fig. 5C,G). Likewise, the cords in SCI + scaffold and SCI with cell seeded scaffold animals showed positive immunostaining for the GAP-43 antibody at the injury site, but unlike their ß-III tubulin staining pattern, cord cells in SCI-only animals were GAP-43 negative (Fig. 5B,F). Cord cells in SCI with cell seeded scaffold group were slightly ß-galactosidase-immunopositive compared

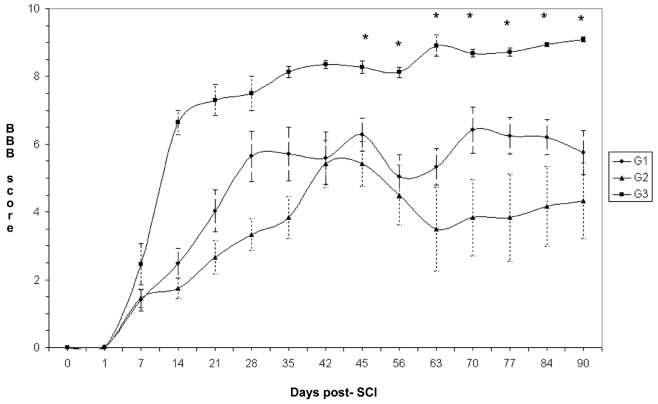

Fig. 3. Motor function improvement in response to the cell-loaded albumin scaffold. Plot shows the scores obtained in the modified BBB locomotor test once a week over 90 days after spinal cord injury and treatment. At all time points from 45 days post-injury, the rate of improvement for G3 was significantly improved over the rate observed in G1 (*$p<0.05$). Values represent the means ± S.E.M. G1: SCI-only. G2: SCI + scaffold. G3: SCI with cell seeded scaffold.

Table 1. Sirius red and immunohistochemical staining results recorded in the three treatment groups.

	SCI-alone	SCI + scaffold	SCI + cell seeded scaffold
Collagen	++	++	++
GFAP	++	-	-
Tyrosine hydroxylase	-	+	+
N-200	-	+	++
Dopamine ß-Hydroxylase	-	-	-
GAP-43	-	+	+++
ß-III-Tubulin	+	+	+++
ß-Galactosidase	-	-	+++

to the control groups, which were both negative for this antibody (Fig. 5D,H).

Discussion

Recent research efforts in the field of SCI therapy have focused on developing new biodegradable scaffolds to act as a permissive and stimulating environment for nerve regeneration (Madigan et al., 2009; Straley et al., 2010). The main goal of the present study was to assess the performance of a solid human serum-derived scaffold developed by our research group. In a previous study, we reported the use of this albumin scaffold to repair bone defects using cultured osteoblasts in a rat

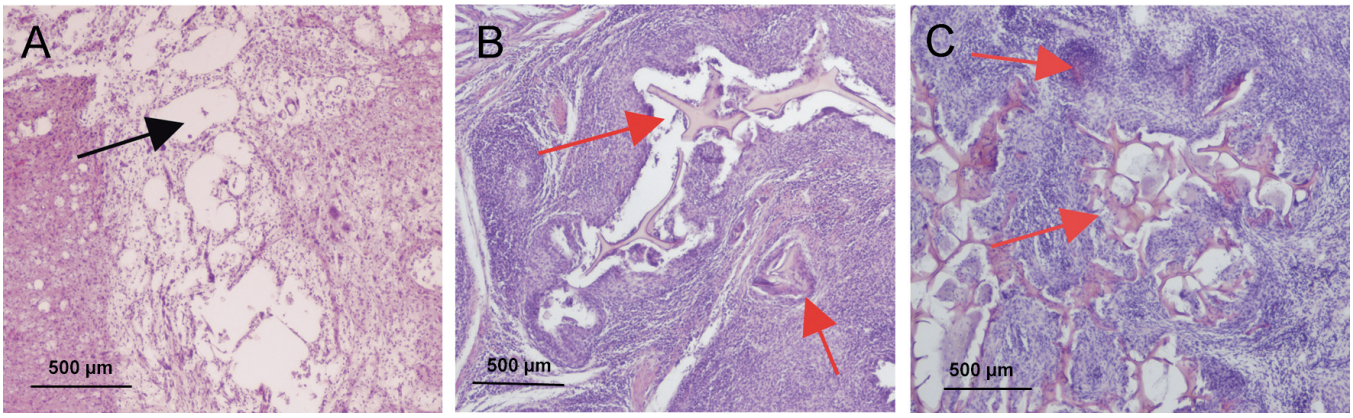

Fig. 4. Hematoxylin/eosin (H&E) staining of 20 µm-thick longitudinal sections of specimens from SCI-only group (G1,A), SCI + scaffold (G2,B), and SCI with cell seeded scaffold group (G3,C). **A.** Histological appearance of the central spinal cord cavity (black arrow) in G1, 90 days after SCI. **B.** Ninety days after SCI and treatment, the spaces at the site of injury were filled with cells. The albumin scaffold (red arrows) was partially degraded and filled with cells. **C.** Ninety days after SCI and treatment, the spaces at the site of injury were filled with ADSCs and OECs. The albumin scaffold (red arrows) was partially degraded and filled with cells.

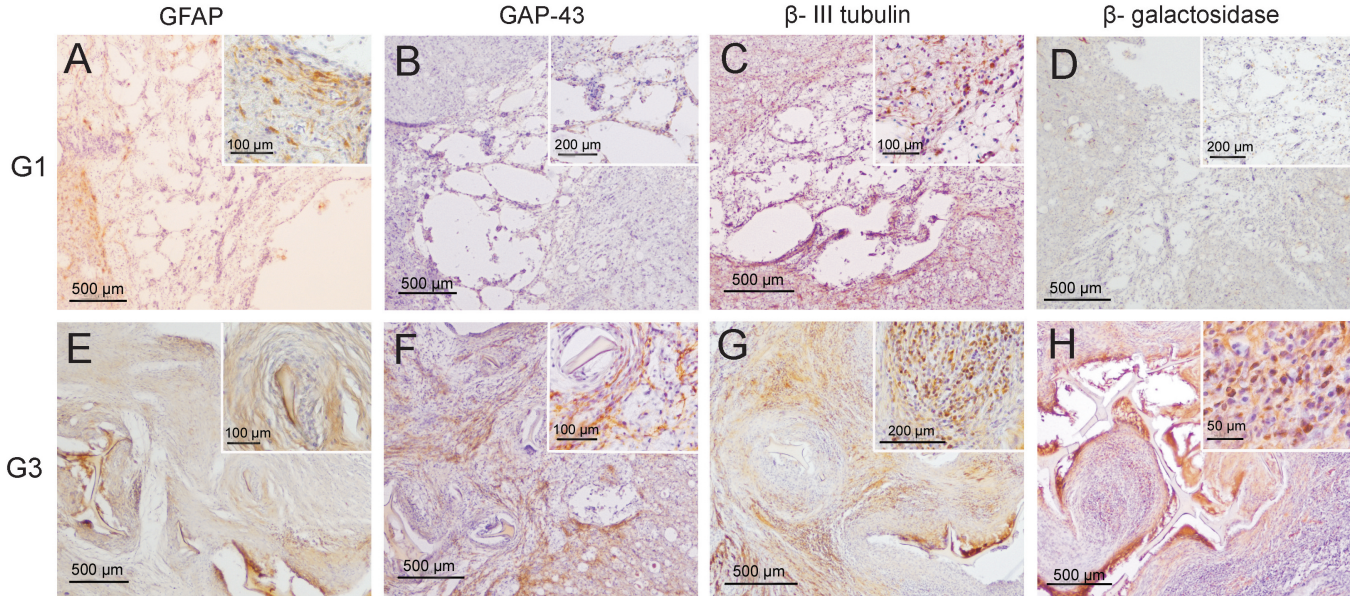

Fig. 5. Immunohistochemical staining of central cord cavities in rats 90 days after SCI and treatment. All sections 20 µm-thick longitudinal. **A-D.** SCI-only group (G1). **E-H.** SCI with cell seeded scaffold group (G3). Note the partially degraded scaffold in these images. **A, E.** Glial cells showing positivity for GFAP can be seen G1 compared to G3. **B, F.** Neuronal cells and fibers showing positivity for GAP-43 can be seen at the injury site within the neoformed tissue in G3 compared to G1. **C, G.** Neuronal cells and fibers showing positivity for ß-III tubulin can be seen at the injury site within the neoformed tissue in G3. Representative longitudinal sections showing positivity for ß-III tubulin in the zones immediately rostral and caudal to the lesion site in G1. **D, H.** Neurons and astroglial cells showing positivity for ß-galactosidase can be seen within the neoformed tissue in G3 compared to G1.

model (Gallego et al., 2010). Similar tissue engineered implants have met with the problem that the toxicity of the crosslinking agent glutaraldehyde usually impairs cell culture. The lyophilization step after crosslinking incorporated in our technique almost eliminates the toxic properties of this agent (Gallego et al., 2010). The findings of this study suggest that the scaffold developed is an appropriate substrate for nerve tissue regeneration and can potentially be used as an autologous scaffold. The scaffold also has the advantage that it is easy and nonexpensive to produce.

Pore structure is very important when considering scaffolds for tissue engineering. High porosity and well-connected pores create good mass transfer properties and increase cell viability. A porous scaffold microstructure with minimal pore size is usually required to allow tissue ingrowth (Zeltinger et al., 2001). The pore size of our scaffold was determined here as ranging from 50 to 150 μm with a larger pore size observed in longitudinal sections than cross sections of scaffold. These pores are thus elongated in shape and highly interconnected, confirming a suitable architecture for cell penetration. Thus, the three-dimensional structure of the scaffold used in our study provides a suitable framework for guiding axon regeneration across its large gaps or cavities, and creates sufficient space for ADSC neuro-transdifferentiation.

Various types of cell have been used in cell therapy approaches to SCI, including Schwann cells (Ramon-Cueto et al., 2000; Verdu et al., 2003; Garcia-Alias et al., 2004) and bone marrow stem cells (BMSCs) (Chopp and Li, 2002; Zurita and Vaquero, 2006). Since harvesting bone marrow (BM) is a highly invasive procedure, researchers have turned to the use of adipose tissue as an alternative rich source of MSC. In effect, ADSCs have numerous properties that make them ideal candidates for cell transplant therapy after SCI. These cells share characteristics with BMSCs, including avoiding immune rejection (Wang et al., 2007), yet they have the advantage that they can be easily obtained from subcutaneous adipose tissue, expanded and stored (Zuk et al., 2001; Yarak and Okamoto, 2010). In contrast, OECs are obtained from the olfactory bulb and olfactory lamina propria with the limitation of the scarce availability of functional cells. Wang et al. (2007) observed that OECs secrete a variety of growth factors that promote the neural differentiation of ADSCs in three-dimensional scaffolds in vitro. Given the complementary biological properties of OECs and ADSCs, we co-transplanted both cell types in our rat model of SCI. Our *in vitro* tests revealed that both OECs and ADSCs maintained their viability and phenotype when used to seed the scaffold. After co-culturing for 7 days in the scaffolds, these were implanted in the injured rats. According to Wang et al. (Wang et al., 2007), *in vivo* neuro-differentiation takes place 20-30 days after implant. The neuro-differentiation of ADSCs and their survival and migration from the implant site will need to be investigated in future studies.

Our functional *in vivo* results are provided as modified BBB walking scores (Basso et al., 1995) recorded in our three experimental groups at 90 days post-injury. Thus, the motor recovery observed in SCI with cell seeded scaffold group (G3) over that recorded in controls at this time point was significant. Other authors (Ramon-Cueto et al., 2000; Lu et al., 2002) have reported that the transplantation of OECs or BMSCs into injured spinal cord tissue in rats with paraplegia promotes a clear functional recovery that starts a few weeks after transplantation (Vaquero et al., 2006). Our SCI with cell seeded scaffold animals showed improved locomotor scores early after SCI (up to 21 days post-injury) over controls (SCI-only, SCI + scaffold), which later stabilized at around 9 (from 45 days post-injury). This score indicates plantar placement of the paw with weight support in stance only or occasional, frequent or consistent weight supported dorsal stepping and no plantar stepping. In contrast, SCI-only group, in which injured animals were left untreated, only achieved stable mean modified BBB scores of approximately 5, and SCI + scaffold group achieved a slightly lower score (approximately 4). These results are consistent with those of several studies (Ramon-Cueto et al., 1998; Deng et al., 2006; Zurita et al., 2008) in which transplantation of either BMSCs or OECs alone was found to promote functional recovery after SCI. Moreover, Deng et al., 2008 described that co-transplantation of OECs and BMSCs could synergistically ameliorate the functional recovery of SCI in rats, probably in such a way that OECs contribute to supporting the neuronal differentiation of implanted BMSCs.

To elucidate possible mechanisms underlying the observed functional recovery, we used several histology and immunohistochemistry techniques. Thus, histological studies on our SCI-untreated control animals revealed the persistence of the typical post-traumatic spinal cord cavity 90 days after injury (Zurita and Vaquero, 2006). In contrast, in the injured animals treated with cell seeded scaffold (G3) or a SCI + scaffold (G2), the post-SCI cavity was completely filled with cells. This suggests that the cells implanted within the scaffold are capable of filling the spinal cord cavity, forming new nervous tissue that could act as a bridge for the passage of descending axons. However, this idea does not explain the infilled spinal cord cavity observed after the implant of the scaffold alone. A possible explanation is that call-cells achieve this by migrating to the lesion site in response to injury. In effect, it is known that these new cells are born (call-cells) in the spinal cord and migrate to the damaged area, where it is assumed they replace injured cells (McDonald and Becker, 2003). Thus, the new scaffold could act as a good support for these call-cells.

The classic concept that scar formation (connective tissue scar or glial scar) in the injured spinal cord tissue might impede the passage of regenerated axons from one extreme of the lesion to the other was histologically and immunohistochemically addressed 90 days after scaffold

implant. At this time point, fibrous tissue identified by Sirius red staining could be seen at the margins of the spinal cord cavity in all the treatment groups. However, immunostaining for GFAP in SCI + scaffold and SCI with cell seeded scaffold groups failed to reveal the presence of astrocytes at the injury site or caudal or rostral to this point 3 months after SCI. At this time point, the tissue repair process has usually reached a steady state. In contrast, large populations of GFAP-positive astrocytes were detected at the injury site and caudal and rostral to this site in SCI-only after SCI. Some authors have reported downregulation of GFAP by reactive astrocytes induced by OECs transplanted into lesioned spinal cords (Verdu et al., 2001). The absence of glial scar tissue observed in the spinal cords of the scaffold-treated animals suggests that the albumin scaffold could directly or indirectly modulate reactive astrocytes, reducing their reactivity and creating a protective environment.

Animals in SCI with cell seeded scaffold group showed immunopositive staining for antibodies against neural and astroglial cells at the injury site, suggesting that the newly formed tissue contains neurons and glial cells. Moreover, this neotissue observed after SCI that completely filled the spinal cord cavity permitted the passage of descending and ascending neurons, as revealed by the specific antibodies used. SCI-only group showed ß-III tubulin-positive fibers suggesting that the slight locomotor recovery observed in control rats could be attributed to the neoformation of the axons detected. Although the scaffold alone is incapable of improving functional recovery, it does seem to be able to inhibit the ingrowth of a variety of cell types, contributing to glial scar inhibition and could also act as a support for call-cells. These results suggest the scaffold itself provides an adequate environment for both the survival and differentiation, at least partly, of these call-cells that fill the cord cavity. Indeed, it has been reported that most of these newborn cells (call-cells) die during the first few weeks because the injured spinal cord does not seem to be a suitable environment (Johansson et al., 1999; Ceccatelli et al., 2004). In contrast, animals undergoing transplant of the scaffold containing both cells types showed significantly improved motor function compared to the remaining animals. Thus, rats in SCI with cell seeded scaffold group that were still alive at 90 days post-injury continued to show recovery, as indicated by their modified BBB scores. Although the scaffold-alone seemed to play a significant role in reducing glial scar formation, the presence of both cells types in the scaffold achieved the greatest recovery. The mechanisms whereby the scaffold plus cells are able to improve the functional recovery process need to be further explored.

In conclusion, our findings indicate that, loaded with OECs and ADSCs, this new human serum-derived spongy scaffold is able to improve motor function recovery in SCI rats and provide future direction for studies designed to test the safety and potential of this scaffold.

Acknowledgements. This work was supported by FICYT PEST 08-12 and Obra Social y Cultural Cajastur. The authors acknowledge the assistance of: Dra. Aurora Astudillo and the staff of pathology unit of the HUCA, Dr. M. Nieto-Sampedro and E. Martín-López, Dra. Ana Martín-Villalba.

References

Arboleda D., Forostyak S., Jendelova P., Marekova D., Amemori T., Pivonkova H., Masinova K. and Sykova E. (2011). Transplantation of predifferentiated adipose-derived stromal cells for the treatment of spinal cord injury. Cell Mol. Neurobiol. 31, 1113-1122.

Balentine J.D. (1978). Pathology of experimental spinal cord trauma. II. Ultrastructure of axons and myelin. Lab. Invest. 39, 254-266.

Barnett S.C. and Riddell J.S. (2004). Olfactory Ensheathing Cells (OECs) and the treatment of CNS injury: advantages and possible caveats. J. Anat. 204, 57-67.

Basso D.M., Beattie M.S. and Bresnahan J.C. (1995). A sensitive and reliable locomotor rating scale for open field testing in rats. J. Neurotrauma 12, 1-21.

Brazda N. and Müller H.W. (2009). Pharmacological modification of the extracellular matrix to promote regeneration of the injured brain and spinal cord. Prog. Brain Res. 175, 269-281.

Busch S.A. and Silver J. (2007). The role of extracellular matrix in CNS regeneration. Curr. Opin. Nerurobiol. 17, 120-127.

Cadelli D.S., Bandtlow C.E. and Schwab M.E. (1992). Oligodendrocyte and myelinassociated inhibitors of neurite outgrowth: their involvement in the lack of CNS regeneration. Exp. Neurol. 115, 189-192.

Ceccatelli S., Tamm C., Sleeper E. and Orrenius S. (2004). Neural stem cells and cell death. Toxicol. Lett. 149, 59-66.

Chopp M. and Li Y. (2002). Treatment of neural injury with marrow stromal cells. Lancet Neurol. 1, 92-100.

Collazos-Castro J.E., Muñeton-Gomez V.C. and Nieto-Sampedro M. (2005). Olfactory glia transplantation into cervical spinal cord contusion injuries. J. Neurosurg. Spine 3, 308-317.

Demjen D., Klussmann S., Kleber S., Zuliani C., Stieltjes B., Metzger C., Hirt U.A., Walczak H., Falk W., Essig M., Edler L., Krammer P.H., Martin-Villalba A. (2004). Neutralization of CD95 ligand promotes regeneration and functional recovery after spinal cord injury. Nat. Med. 10, 389-395.

Deng Y.B., Liu X.G., Liu Z.G., Liu X.L., Liu Y. and Zhou G.Q. (2006). Implantation of BM mesenchymal stem cells into injured spinal cord elicits de novo neurogenesis and functional recovery: evidence from a study in rhesus monkeys. Cytotherapy 8, 210-214.

Deng Y.B., Liu Y., Zhu W.B., Bi X.B., Wang Y.Z., Ye M.H. and Zhou G.Q. (2008). The co-transplantation of human bone marrow stromal cells and embryo olfactory ensheathing cells as a new approach to treat spinal cord injury in a rat model. Cytotherapy 10, 551-564.

Fawcett J.W. and Asher R.A. (1999). The glial scar and central nervous system repair. Brain Res. Bull. 49, 377-391.

Gallego L., Junquera L., Meana A., Alvarez-Viejo M. amd Fresno M. (2009). Ectopic bone formation from mandibular osteoblasts cultured in a novel human serum-derived albumin scaffold. J. Biomater. Appl. 25, 367-381.

Gallego L., Junquera L., Garcia E., Garcia V., Alvarez-Viejo M., Costilla S., Fresno M.F. and Meana A. (2010). Repair of rat mandibular bone

defects by alveolar osteoblasts in a novel plasma-derived albumin scaffold. Tissue Eng. 16, 1179-1187.

Garcia-Alias G., Lopez-Vales R., Fores J., Navarro X. and Verdu E. (2004). Acute transplantation of olfactory ensheathing cells or Schwann cells promotes recovery after spinal cord injury in the rat. J. Neurosci. Res. 75, 632-641.

Groves A.K., Barnett S.C., Franklin R.J., Crang A.J., Mayer M., Blakemore W.F. and Noble M. (1993). Repair of demyelinated lesions by transplantation of purified O-2A progenitor cells. Nature 362, 453-455.

Gudiño-Cabera G. and Nieto-Sampedro M. (1996). Ensheathing cells: Large scale purification from adult olfactory bulb, freeze-preservation and migration of transplanted cells in adult brain. Rest. Neurol. Neurosci. 10, 25-34.

Jin K., Mao X.O., Batteur S., Sun Y. and Greenberg D.A. (2003). Induction of neuronal markers in bone marrow cells: differential effects of growth factors and patterns of intracellular expression. Exp. Neurol. 84, 78-89.

Johansson C.B., Momma S., Clarke D.L., Risling M., Lendahl U. and Frisen J. (1999). Identification of a neural stem cell in the adult mammalian central nervous system. Cell. 96, 25-34.

Kang S.K., Lee D.H., Bae Y.C., Kim H.K., Baik S.Y. and Jung J.S. (2003). Improvement of neurological deficits by intracerebral transplantation of human adipose tissue-derived stromal cells after cerebral ischemia in rats. Exp. Neurol. 183, 355-366.

Li C., Li L., Zhe-Yu C., Li-Mei W., Jun-LI Y., Hai-Yan Q., Chang-Lin L. and Cheng H. (2004). Olfactory ensheating cells genetically modified to secrete GDNF to promote spinal cord repair. Brain 127, 535-549.

Lu J., Feron F., Mackay-Sim A. and Waite P.M. (2002). Olfactory ensheathing cells promote locomotor recovery after delayed transplantation into transected spinal cord. Brain 125, 14-21.

Madigan N.N., McMahon S., O'Brien T., Yaszemski M.J. and Windebank A.J. (2009). Current tissue engineering and novel therapeutic approaches to axonal regeneration following spinal cord injury using polymer scaffolds. Respir. Physiol. Neurobiol. 169, 183-199.

McDonald J.W. and Becker D. (2003). Spinal cord injury: promising interventions and realistic goals. Am. J. Phys. Med. Rehabil. 82, S38-49.

McGee A.W. and Strittmatter S.M. (2003). The Nogo-66 receptor: focusing myelin inhibition of axon regeneration. Trends Neurosci. 26, 193-198.

Meana A., Garcia E., Garcia V., Jorcano J.L., del Rio M., Larcher F., Duarte B. and Holguin A. (2008). Method for preparing three-dimensional structures for tissue engineering. WO/2008/119855.

Olson H.E., Rooney G.E., Gross L., Nesbitt J.J., Galvin K.E., Knight A., Chen B., Yaszemski M.J. and Windebank A.J. (2009). Neural stem cell- and Schwann cell-loaded biodegradable polymer scaffolds support axonal regeneration in the transected spinal cord. Tissue Eng. Part A. 15, 1797-1805.

Radtke C., Aizer A.A., Agulian S.K., Lankford K.L., Vogt P.M. and Kocsis J.D. (2009). Transplantation of olfactory ensheathing cells enhances peripheral nerve regeneration after microsurgical nerve repair. Brain Res. 1254, 10-17.

Raisman G. (1985). Specialized neuroglial arrangement nay explain the capacity of vomeronasal axons to reinnervate central neurons. Neuroscience. 14, 237-254.

Raisman G. (2001). Olfactory ensheathing cells-another miracle cure for spinal cord injury? Nat. Rev. Neurosci. 2, 369-375.

Ramon-Cueto A. and Nieto-Sampedro M. (1994). Regeneration into the spinal cord of transected dorsal root axons is promoted by ensheathing glia transplants. Exp. Neurol. 127, 232-244.

Ramon-Cueto A., Plant G.W., Avila J. and Bunge M.B. (1998). Long-distance axonal regeneration in the transected adult rat spinal cord is promoted by olfactory ensheathing glia transplants. J. Neurosci. 18, 3803-3815.

Ramon-Cueto A., Cordero M.I., Santos-Benito F.F. and Avila J. (2000). Functional recovery of paraplegic rats and motor axon regeneration in their spinal cords by olfactory ensheathing glia. Neuron 25, 425-435.

Resnick D.K., Cechvala C.F., Yan Y., Witwer B.P., Sun D. and Zhang S. (2003). Adult olfactory ensheating cell transplantation for acute spinal cord injury. J. Neurotrauma 20, 279-285.

Schwab M.E. and Caroni P. (2008). Antibody against myelin-associated inhibitor of neurite growth neutralizes nonpermissive substrate properties of CNS white matter. Neuron 60, 404-405.

Straley K.S., Foo C.W. and Heilshorn S.C. (2010). Biomaterial design strategies for the treatment of spinal cord injuries. J. Neurotrauma 27, 1-19.

Tatard V.M., D'Ippolito G., Diabira S., Valeyev A., Hackman J., McCarthy M., Bouckenooghe T., Menei P., Montero-Menei C.N. and Schiller P.C. (2007). Neurotrophin-directed differentiation of human adult marrow stromal cells to dopaminergic-like neurons. Bone 40, 360-373.

Vaquero J., Zurita M., Oya S. and Santos M. (2006). Cell therapy using bone marrow stromal cells in chronic paraplegic rats: systemic or local administration? Neurosci. Lett. 398,129-134.

Verdu E., Garcia-Alias G., Fores J., Gudiño-Cabrera G., Muñeton V.C., Nieto-Sampedro M. and Navarro X. (2001). Effects of ensheating cells transplanted into photochemically damaged spinal cord. Neuroreport 12, 2303-2309.

Verdu E., Garcia-Alias G., Fores J., Lopez-Vales R. and Navarro X. (2003). Olfactory ensheathing cells transplanted in lesioned spinal cord prevent loss of spinal cord parenchyma and promote functional recovery. Glia 42, 275-286.

Wang B., Zhao Y., Lin H., Chen B., Zhang J., Zhang J., Wang X., Zhao W. and Dai J. (2006). Phenotypical analysis of adult rat olfactory ensheathing cells on 3-D collagen scaffolds. Neurosci. Lett. 401, 65-70.

Wang B., Han J., Gao Y., Xiao Z., Chen B., Wang X., Zhao W. and Dai J. (2007). The differentiation of rat adipose-derived stem cells into OEC-like cells on collagen scaffolds by co-culturing with OECs. Neurosci. Lett. 421, 191-196.

Yarak S. and Okamoto O.K. (2010). Human adipose-derived stem cells: current challenges and clinical perspectives. An. Bras. Dermatol. 85, 647-656.

Zeltinger J., Sherwood J.K., Graham D.A., Müeller R. and Griffith L.G. (2001). Effect of pore size and void fraction on cellular adhesion, proliferation, and matrix deposition. Tissue Eng. 7, 557-572.

Zhang L., Ma Z., Smith G.M., Wen X., Pressman Y., Wood P.M. and Xu X.M. (2009). GDNF-enhanced axonal regeneration and myelination following spinal cord injury is mediated by primary effects on neurons. Glia 57, 1178-1191.

Zuk P.A., Zhu M., Mizuno H., Huang J., Futrell J.W., Katz A.J., Benhaim P., Lorenz H.P. and Hedrick M.H. (2001). Multilineage cells from human adipose tissue: implications for cell-based therapies. Tissue Eng. 7, 211-228.

Zurita M. and Vaquero J. (2006). Bone marrow stromal cells can achieve cure of chronic paraplegic rats: functional and morphological outcome one year after transplantation. Neurosci. Lett. 402, 51-56.

Zurita M., Vaquero J., Bonilla C., Santos M., De Haro J., Oya S. and Aguado C. (2008). Functional recovery of chronic paraplegic pigs after autologous transplantation of bone marrow stromal cells. Transplantation 86, 845-853.

Accepted July 11, 2012